Hindawi Publishing Corporation
Journal of Polymers
Volume 2014, Article ID 906780, 9 pages
http://dx.doi.org/10.1155/2014/906780

Research Article

Role of Hard-Acid/Hard-Base Interaction on Structural and Dielectric Behavior of Solid Polymer Electrolytes Based on Chitosan-XCF_3SO_3 ($X = Li^+, Na^+, Ag^+$)

Shujahadeen B. Aziz[1] and Zul Hazrin Z. Abidin[2]

[1] *Department of Physics, Faculty of Science and Science Education, University of Sulaimani, Sulaimani City, Kurdistan Regional Government, Iraq*
[2] *Centre for Ionics University of Malaya (CIUM), Department of Physics, Faculty of Science, University of Malaya, 50603 Kuala Lumpur, Malaysia*

Correspondence should be addressed to Shujahadeen B. Aziz; shujaadeen78@yahoo.com

Received 6 August 2013; Accepted 17 December 2013; Published 16 January 2014

Academic Editor: Jean-Marc Saiter

Solid films of pure chitosan, chitosan-$LiCF_3SO_3$, chitosan-$NaCF_3SO_3$, and chitosan-$AgCF_3SO_3$ were prepared using solution cast technique. The influence of cation size on the chitosan structure has been investigated by X-ray diffraction technique. The interaction between the alkali metal ions and the donor atoms of chitosan polymer is a strong hard-acid/hard-base interaction. It was found that the intensity of crystalline peaks of chitosan decreases with increase of cation size. The impedance analysis shows that ionic transport is high for the high amorphous system. The second semicircle in Z''-Z' plots and the surface plasmonic resonance (SPR) peaks in chitosan-$AgCF_3SO_3$ sample system reveal the formations of silver metal nanoparticles. It was found that the high amorphous sample exhibits the high dielectric constant and dielectric loss values. The increase of dielectric constant and dielectric loss with temperature for chitosan-salt membranes indicated an increase of charge carrier concentration.

1. Introduction

Polymer electrolytes may be defined as a membrane having enhanced transport properties comparable with that of the common liquid ionic solution. The conductivity of these polymers can be controlled by changing their redox state by means of chemical or electrochemical reduction or oxidation accompanied by insertion of counter ion [1]. Due to the advantages that polymer electrolytes offer over conventional materials, including no internal shorting, leakage of electrolytes, ease of processing, productivity, and cost reduction [2]. In addition, polymer electrolytes possess the advantage of flexibility over inorganic solids [3]. Amorphous solid electrolytes (polymer salt complexes) have gained technological importance for their possible applications in a variety of devices such as lithium batteries, fuel cells, electrochromic displays, supercapacitors, and sensors [4–6]. Polymer electrolytes usually contain both crystalline and amorphous phases. It has been reported that the ion conduction takes place primarily in the amorphous phase [7].

Chitosan is a biocompatible and biosorbable biopolymer which is currently receiving a great deal of interest for medical and pharmaceutical applications due to its interesting intrinsic properties [8] and it is a polycationic polymer due to the existence of one amino group and two hydroxyl groups in their repeating units [9]. It is well known that chitosan is an outstanding sorbent of extremely high affinity for transition metal ions due to the abundance of polar groups (NH_2 and OH) in chitosan chains which served as conjunction sites [10]. An important feature of chitosan is its ability to be molded in various forms, such as films, porous scaffolds, and hydrogels [11].

From the fundamental point of view, dielectric relaxation and ion conduction mechanism in solids are the most intensively researched topics in condensed matter physics and especially ionic transport in polymer electrolytes is

a complicated subject and not completely understood. Ion transport is complex and depends on factors such as salt concentration, dielectric constant of host polymer, degree of salt dissociation and ion aggregation, and mobility of polymer chains [12–15]. It was reported, that in polymer electrolytes containing inorganic salts as a dopant, the decrease in XRD intensity of the host polymer is directly related to the dominance of amorphous nature of the solid polymer electrolyte sample; that, is a higher conductivity is associated with more amorphous system [16, 17]. Khulbe et al. [18] used the X-ray diffraction technique to investigate the effect of different solvent on the crystalline nature of dense PPO solid film. To our knowledge, there is no report in the literature about the effect of cation size on structural behavior of chitosan based polymer electrolyte. In the present paper three different salts such as $AgCF_3SO_3$, $NaCF_3SO_3$ and $LiCF_3SO_3$ have been used to prepare chitosan based solid electrolytes.

The main objective of the present work is to investigate the effect of cationic size on structural and electrical behaviors of chitosan based solid polymer electrolyte. The X-ray diffraction (XRD) and electrical impedance spectroscopy (EIS) have been used to characterize chitosan based polymer electrolytes. The frequency range employed for the measurements was typically 50 Hz to 1 M Hz.

2. Experimental Details

2.1. Materials and Sample Preparation. Solution cast technique was used to prepare chitosan based polymer electrolyte membranes. $AgCF_3SO_3$, $NaCF_3SO_3$, $LiCF_3SO_3$ and chitosan (from crab shells; ≥75% deacetylated, Sigma Aldrich) have been used as the raw materials in this study. One gram of chitosan was dissolved in 100 mL of 1% acetic acid solution. The mixture was stirred continuously with magnetic stirrer for several hours at room temperature until the chitosan powder has completely dissolved. To this set of solutions 10 wt. % of $AgCF_3SO_3$, $NaCF_3SO_3$, and $LiCF_3SO_3$ was added separately and the mixtures were stirred continuously until homogeneous solutions were obtained. These solutions were then cast into different plastic petridish and left to dry at room temperature in order to allow complete evaporation of the solvent. The membrane films were kept in desiccators with silica gel desiccant for further drying process.

2.2. X-Ray Diffraction. In this paper, XRD was performed to study the nature of complexation between $AgCF_3SO_3$, $NaCF_3SO_3$, $LiCF_3SO_3$, and chitosan. XRD was carried out using X-ray diffractometer (Bruker AXS) with operating voltage and current of 40 kV and 40 mA, respectively. The membrane films were scanned with a beam of monochromatic radiation of wavelength $\lambda = 1.5406$ Å and the glancing angles were in the range of $5^\circ \leq 2\theta \leq 80^\circ$ with a step size of 0.1°.

2.3. Impedance Measurement. Complex impedance spectroscopy is the currently used technique. This study gives information on electrical properties of materials and their interface with electronically conducting electrodes. The complex impedance spectroscopy measurement of a.c. conductivity is based on studies made on the measurement of cell impedance/admittance over a range of temperatures and frequencies and analyzing them in complex impedance plane. Impedance is a more general concept than resistance because it takes phase differences into account. In a.c., the resistance, R, is replaced by the impedance, Z, which is the sum of resistance (Z') and reactance (Z'') [19]. The solid polymer electrolyte (SPE) membranes were cut into small discs (2 cm diameter) and sandwiched between two stainless steel electrodes under spring pressure. The impedance of the films was measured using the HIOKI 3531 Z Hi-tester (made in Japan, No. 1036555) that was interfaced to a computer in the frequency range from 50 Hz to 1 M Hz. The software controls the measurements and calculates the real and imaginary parts of impedance. The real (Z') and imaginary (Z'') part of complex impedance (Z^*) were used for calculation of the real and imaginary parts of complex permittivity (ε^*), using the following relations [20, 21]

$$Z^* = Z' - jZ'',$$
$$\varepsilon^* = \varepsilon' - j\varepsilon'' = \frac{1}{j\omega\varepsilon_\circ Z^*}. \quad (1)$$

From (1) one can get the following relation:

$$\varepsilon' = \frac{Z''}{\omega\, C_\circ \left(Z'^2 + Z''^2\right)},$$
$$\varepsilon'' = \frac{Z'}{\omega\, C_\circ \left(Z'^2 + Z''^2\right)}. \quad (2)$$

Here $C_\circ$ is the vacuum capacitance and given by $\varepsilon_\circ A/t$, where t is the thickness and A is active area of the film. The angular frequency ω is equal to $\omega = 2\pi f$, where f is the frequency of the applied field.

2.4. UV-Vis Measurement. The UV-vis spectra of the chitosan-silver triflate membrane film have been recorded using a Jasco V-570 UV-Vis-NIR spectrophotometer (Japan, Jasco SLM-468) in the absorbance mode.

3. Results and Discussion

3.1. X-Ray Diffraction Analysis. X-ray diffraction (XRD) studies can provide a wide range of information on crystal structure, crystal orientation, crystallinity, crystallite size, and phase changes of materials which are characterized by the presence of sharp diffraction rings or peaks [22]. For the present study the X-ray diffraction technique has been used to demonstrate the complex formation between the chitosan polymer and salts and to investigate the effect of cationic size on the crystalline structure of chitosan-based polymer electrolytes. X-ray diffraction (XRD) analysis for pure chitosan film, $LiCF_3SO_3$, $NaCF_3SO_3$, $AgCF_3SO_3$, and their complexes has been performed. Figures 1(a)–1(c) show the X-ray diffraction patterns of the salts, $LiCF_3SO_3$, $NaCF_3SO_3$, and $AgCF_3SO_3$.

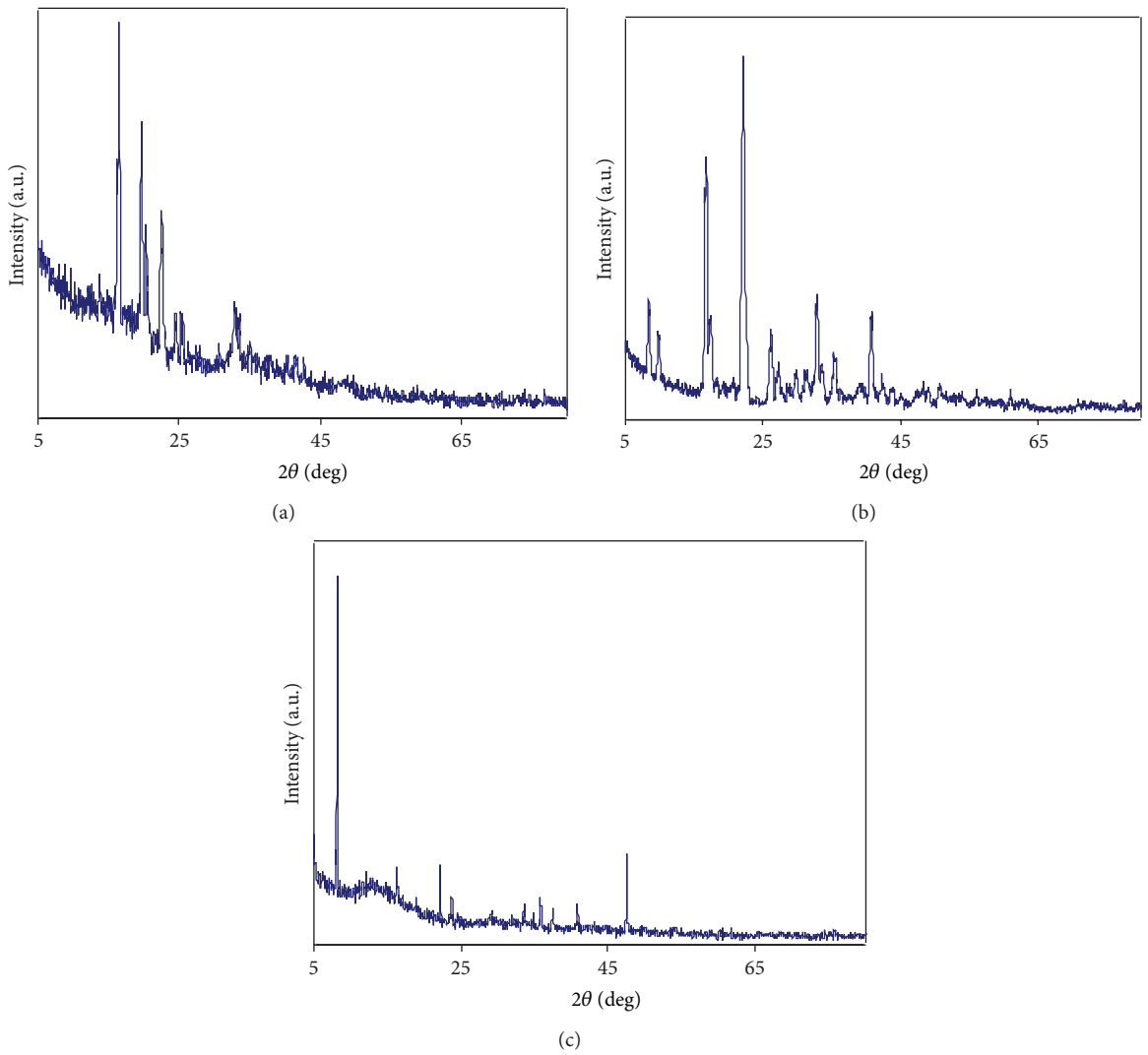

FIGURE 1: X-ray diffraction pattern of (a) $LiCF_3SO_3$, (b) $NaCF_3SO_3$, and (c) $AgCF_3SO_3$.

From the XRD results, one can see that the crystalline peaks of lithium triflate salt are located at $2\theta^\circ = 16.5^\circ, 19.75^\circ, 20.4^\circ, 22.55^\circ, 25.3^\circ$, and 33.15°, whilst for the sodium triflate salt these peaks have been observed at $2\theta^\circ = 8.5^\circ, 9.95^\circ, 16.8^\circ, 22.15^\circ, 26.25^\circ, 32.9^\circ, 35.6^\circ$, and 40.9°, as well as at $2\theta^\circ = 8.2^\circ, 16.3^\circ, 22.2^\circ, 23.7^\circ, 40.8^\circ$, and 47.5° for the silver triflate salt.

Upon mixing the salts with chitosan host polymer separately, and due to the occurrence of complex formation between the chitosan polymer and salts, a serious change in the structural form has been detected as shown in Figure 2(a–d).

It is well known that pure chitosan membrane possesses semicrystalline structure as our results have also supported this fact. In the XRD pattern of pure chitosan, the broad peaks at around $2\theta^\circ = 15^\circ$ and 20° indicate the average intermolecular distance of the crystalline part of pure chitosan membrane [23]. The rigid crystalline structure of chitosan is maintained by intramolecular and intermolecular hydrogen bond which is established by an amino and hydroxyl groups through an absorbed water molecule [24]. It can be observed (see Figure 2(b)) that, with addition of 10 wt. % $LiCF_3SO_3$, the diffraction pattern is looking almost the same like that of

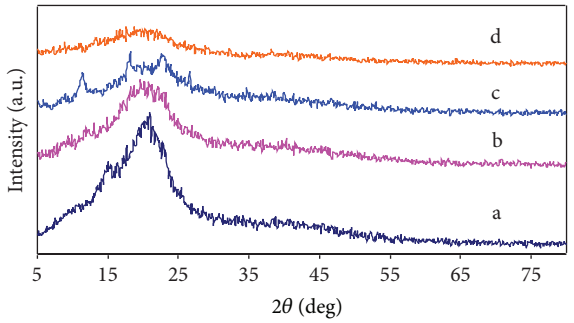

FIGURE 2: X-ray diffraction pattern of (a) pure chitosan, (b) chitosan: 10 wt. % $LiCF_3SO_3$, (c) chitosan: 10 wt. % $NaCF_3SO_3$, and (d) chitosan: 10 wt. % $AgCF_3SO_3$.

pure chitosan membrane but with relatively low intensity of the crystalline peaks. However, adding 10 wt. % of $NaCF_3SO_3$ to chitosan (Figure 2(c)) has partially made the crystalline peaks of pure chitosan disappear. This can be attributed to the elimination of hydrogen bonding between amino groups and hydroxyl groups as a result of complex formation between chitosan and sodium triflate; that is, the amorphous phase dominates the sample with only a few crystalline peaks being present [25]. These new peaks at $2\theta^\circ = 8.5^\circ, 18.3^\circ$, and 23° in X-ray diffractogram of chitosan: $NaCF_3SO_3$ (Figure 2(c)) may be due to some sort of a long-range order set by the presence of ion multiples [26]. But Sanders et al. ascribed such peaks to the formation of polymer-salt complexes rather than pure sodium triflate salt [27].

Interestingly, an increase in broadness and a complete decrease in the intensity at $2\theta^\circ = 20^\circ$ peak for pure chitosan have been observed in the chitosan: $AgCF_3SO_3$ membrane (see Figure 2(d)). As compared to other membranes, chitosan: $AgCF_3SO_3$ membrane showed the most amorphous sample and possessed the highest conductivity value. These results are in good agreement with those made by Hema et al. [28] as they showed that the intensity of XRD pattern decreases with increase in amorphous nature. In other words, the increase in amorphous nature results in greater ionic diffusivity and enhances the ionic conductivity [29]. There is no new peaks that have been observed in the X-ray diffractogram of chitosan: $AgCF_3SO_3$ membrane, showing that the silver triflate salt has completely dissolved in the chitosan. This provides us with the interesting fact that the decrease in crystallinity of chitosan based membranes strongly depends on the cationic sizes, that is, Li^+, Na^+, and Ag^+. Since the ionic radius of Ag^+ ($r = 1.26$ Å) is much greater than Na^+ ($r = 0.95$ Å) and Li^+ ($r = 0.60$ Å), the crystallinity of chitosan-salt membranes can only disrupt $AgCF_3SO_3$ as compared to lithium and sodium triflates. According to Pearson's Hard-Soft-Acid-Base (HSAB) theory [30], Ag^+ is a soft cation and Li^+ is a hard cation. Large, highly polarizable, easily oxidized, and low electronegativity ions are soft, while those that are small, difficult to polarize, not easily oxidized, and highly electronegative are hard. A strong bond is formed between hard cation and hard anion and a weak bond is formed between a soft cation and a hard anion. Chitosan like polyethylene oxide (PEO) has donor atoms (Oxygen and Nitrogen) with high electronegativity and low polarizability and are, therefore, hard bases [31]. As a result, Ag^+ and Na^+ ions interact weakly with the donor atoms of the chitosan host polymer but Li^+ ion can form strong bonds with the donor atoms [30, 31]. This is because Li^+ can be easily solvated and accommodate in the chitosan structure without sacrificing the crystallinity. While as, due to large cation size of Ag^+ and Na^+, they cannot fit into the chitosan crystal structure, which leads to loss of polymer crystallinity. Thus, from the above results we conclude that chitosan: $AgCF_3SO_3$ sample exhibits high amorphous nature comparing to that of the other two systems. We believe that these noticeable good results obtained for chitosan: $AgCF_3SO_3$ sample will nominate the system to be used as a solid polymer film for gas separation as most polymer membranes used for gas separation are of high amorphous or low crystalline structure [18].

3.2. Impedance (Z^*) and UV-Vis Spectroscopy Measurements. To get more insight into our investigated polymer electrolytes, an impedance measurement was carried out. The complex impedance plots (Z'' versus Z') are commonly used to separate the bulk material (depressed semicircle) and the electrode surface polarization phenomena (tilted spike) [32]. The electrode polarization phenomena (tilted spike) occurs due to formation of electric double layer (EDL) capacitances by the free charges build up at the interface between the electrolyte and the electrode surfaces in plane geometry [32, 33]. The intercept of the semicircle with the real axis (Z') at low frequency (end) gives rise to the bulk (ionic) resistance (R_b) of the materials. A common feature of dielectrics with dc conductivity is a discontinuity at electrode/solid dielectric interface, which has different polarization properties than the bulk dielectric. The complex impedance plots at 308 K, which are demonstrated in Figures 3(a)–3(c), strongly supported our XRD results. It is clear that the bulk resistance for chitosan: $LiCF_3SO_3$ ($4.175 \times 10^5\ \Omega$) and chitosan: $NaCF_3SO_3$ ($2.14 \times 10^5\ \Omega$) is higher than that of chitosan: $AgCF_3SO_3$ membrane ($2.3 \times 10^4\ \Omega$). In other words, the bulk conductivity of chitosan: $AgCF_3SO_3$ membrane was larger comparing to that of chitosan: $LiCF_3SO_3$ and chitosan: $NaCF_3SO_3$ membranes; that is, the high amorphous membrane exhibits high ionic diffusivity (ionic transport) [29].

Figures 4(a)–4(c) show the impedance plots for the chitosan salt membranes at 348 K. It is obvious that the radiuses of the semicircles for chitosan salt membranes are decreased with increase in temperature which can be attributed to the increase in conductivity. It can be noticed that chitosan-$AgCF_3SO_3$ membrane (Figure 4(c)) exhibits two semicircles compared to other two membranes. The first semicircle (small semicircle) can be attributed to the bulk conductivity, while the second semicircle can be ascribed to the presence of silver nanoparticles. This phenomenon can be more understood by taking the UV-Vis spectra of chitosan-$AgCF_3SO_3$. The variation in bulk resistance (bulk conductivity) for chitosan-salt system at this low salt concentration can be interpreted by identifying two main factors, which control the ionic mobility [34]. Firstly, cations with smaller radii exhibit stronger interaction with the polar groups (electron donating groups) of the polymer backbone, resulting in more inert bonds which decrease the mobility of the cation and thus the lower conductivity. Secondly, smaller cations are expected to coordinate with fewer polar groups and therefore more polar groups will be left uncoordinated at a given composition. This is expected to result in faster average segmental motions for the smaller cations. These two factors influence the conductivity in different direction. The second factor, the difference in the number of polar groups coordinated by the cations, can be expected to dominate at high salt concentrations [34]. The first factor, the difference in bond labiality, can be expected to increase in importance at lower salt concentrations. Therefore, the present impedance

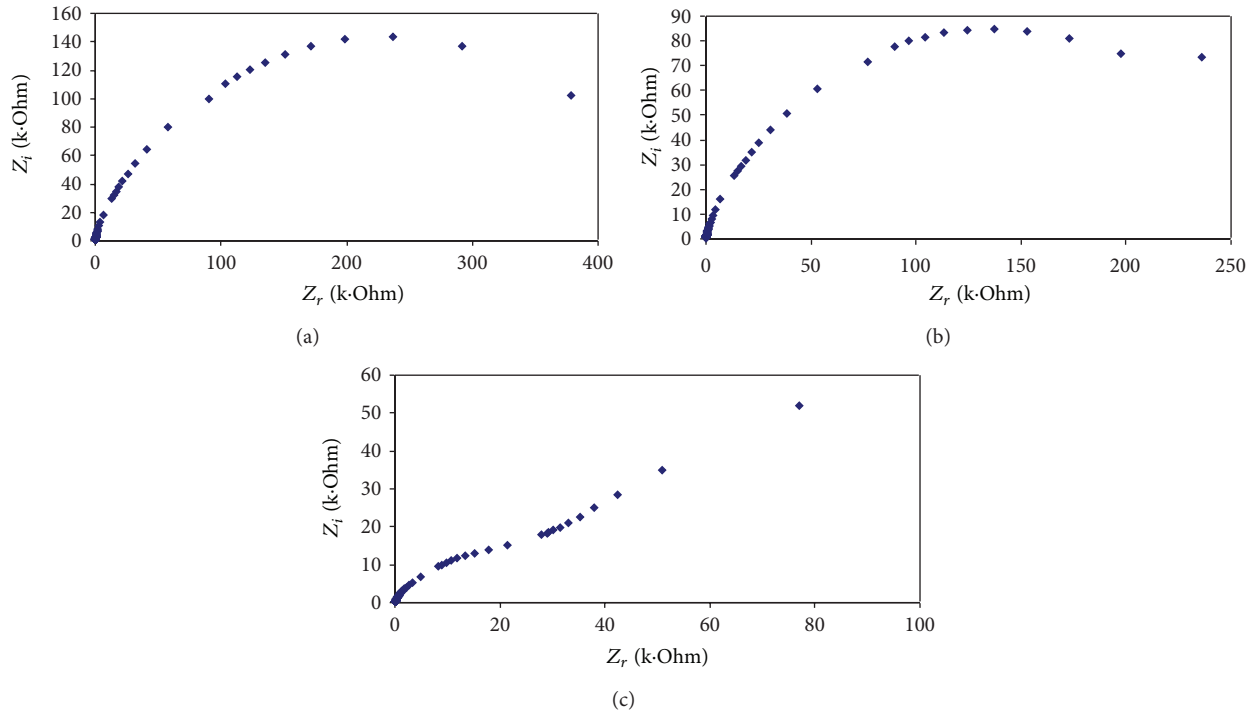

FIGURE 3: Cole-Cole plots for (a) chitosan: $LiCF_3SO_3$, (b) chitosan: $NaCF_3SO_3$, and (c) chitosan-$AgCF_3SO_3$ at 308 K.

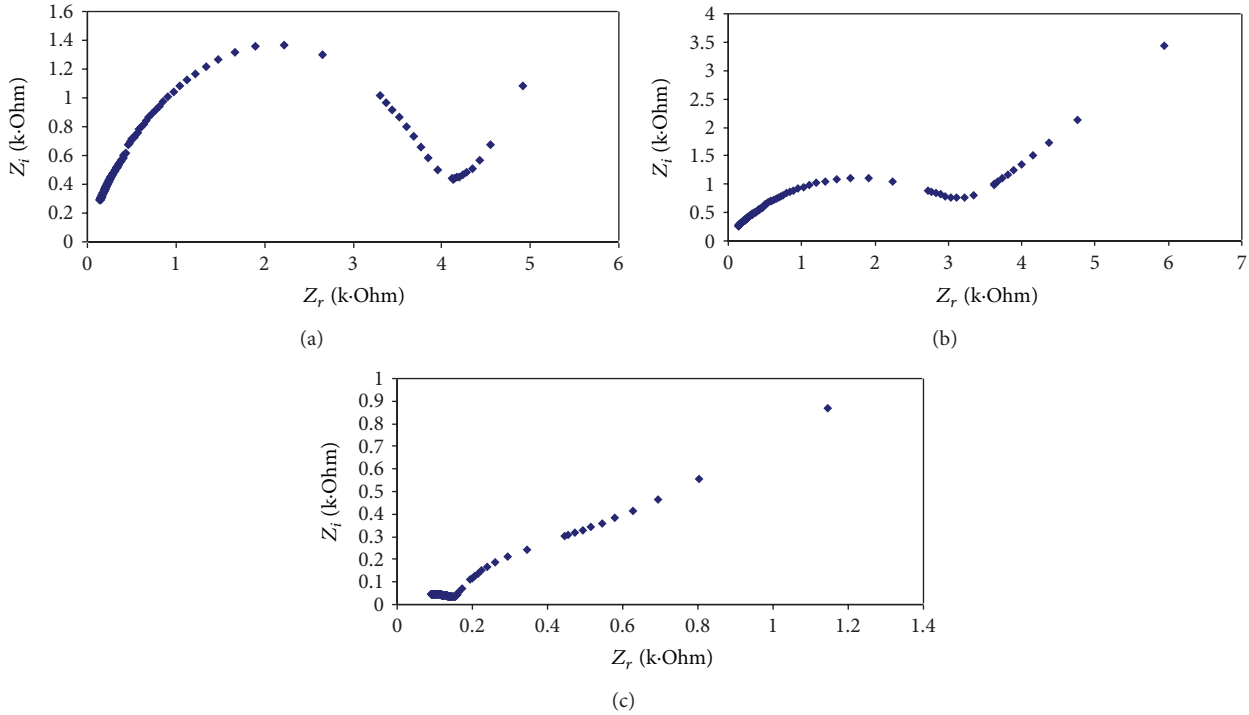

FIGURE 4: Cole-Cole plots for (a) chitosan: $LiCF_3SO_3$, (b) chitosan: $NaCF_3SO_3$, and (c) chitosan-$AgCF_3SO_3$ at 348 K.

behavior is in a good agreement with first factor interpretation and strongly supported by X-ray diffraction analysis (Figure 2(a–d)).

To investigate the formation of silver metal nanoparticle in chitosan: $AgCF_3SO_3$ membrane, UV-vis technique was employed as a common characterizing method. Kang et al. reported that polar polymer solvents can reduce silver ion to silver metal nanoparticle [35]; this is because silver ions are easily reduced by the lone pair electrons of the polar groups (nitrogen and oxygen) [36]. Figure 5 shows

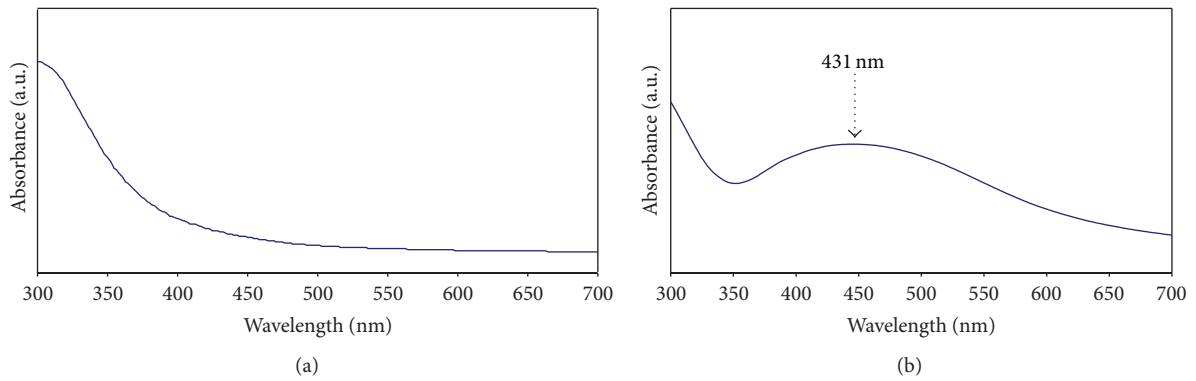

FIGURE 5: UV-vis absorption spectra of (a) pure chitosan and (b) chitosan: $AgCF_3SO_3$ at ambient temperature.

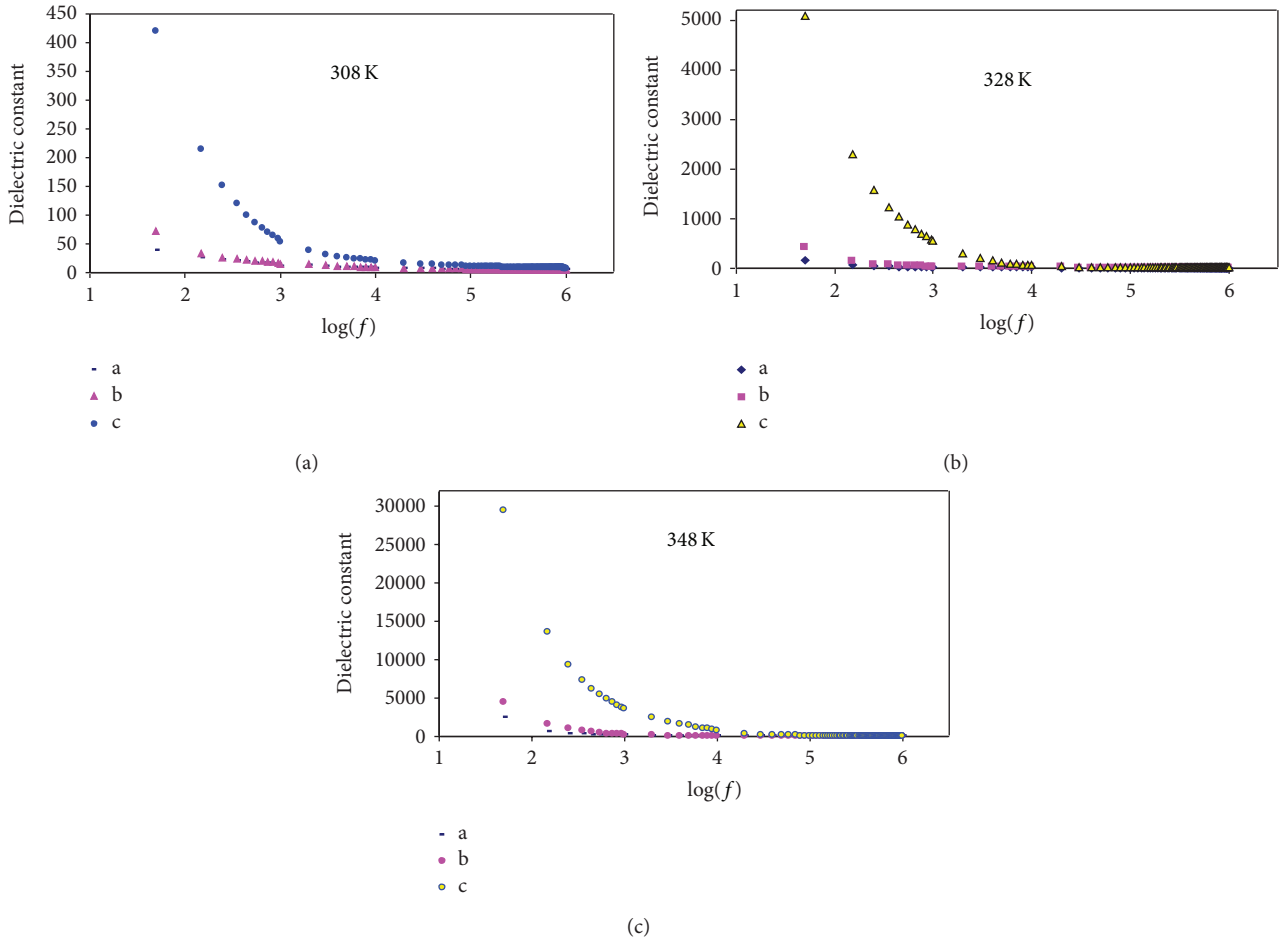

FIGURE 6: Frequency dependence of dielectric constant (ε') at different temperature for (a) chitosan-$LiCF_3SO_3$, (b) chitosan-$NaCF_3SO_3$, and (c) chitosan-$AgCF_3SO_3$.

the UV-vis absorption spectra of pure chitosan and chitosan: $AgCF_3SO_3$ electrolyte at ambient temperature.

It can be seen from the figure that pure chitosan has no absorption peak in the region 400 nm to 500 nm, while a broad absorption peak with a maximum at 426 nm was observed for chitosan: $AgCF_3SO_3$, which can be attributed to the surface plasmon band of silver nanoparticles. It is confirmed that the absorption peak whose maximum occurs at around 420 nm is related to the formation of metallic silver nanoparticles and the peak intensity gives information on the nanoparticles concentrations [37–39]. Thus, UV-vis analysis reveals that the appearance of second semicircle in the electrical impedance plots of chitosan: $AgCF_3SO_3$ system is attributable to the formation of silver nanoparticles. Consequently both UV-vis and impedance analysis confirm the existence of silver nanoparticles.

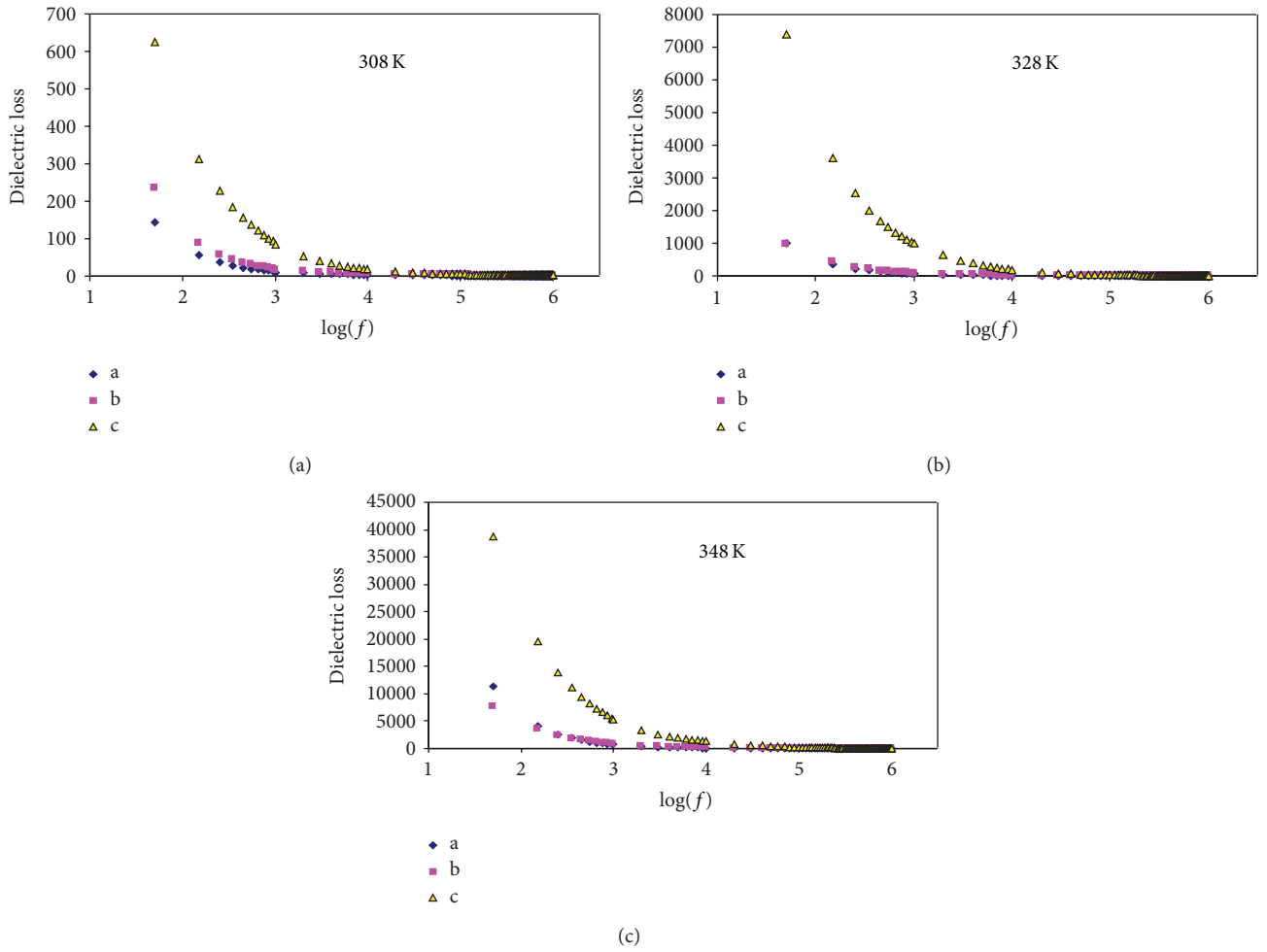

FIGURE 7: Frequency dependence of dielectric loss (ε') at different temperatures for (a) chitosan-$LiCF_3SO_3$, (b) chitosan-$NaCF_3SO_3$, and (c) chitosan-$AgCF_3SO_3$.

3.3. Dielectric Analysis. The ion transport in polymer electrolyte can be understood from dielectric analysis [40]. Hence, it becomes important to understand the ion conduction mechanism along with polymer segmental relaxation processes in polymer electrolyte. Therefore, the study of dielectric properties can be used to understand the ion transport behavior and to obtain the information of ionic/molecular interaction in solid polymer electrolyte [41]. The complex permittivity function, $\varepsilon^*(\omega) = \varepsilon'(\omega) + \varepsilon''(\omega)$, is a materials property depending on frequency of the applied field, temperature, humidity, structure, and other external factors, where $\varepsilon'(\omega)$ is related to the energy stored in the material and $\varepsilon''(\omega)$ is proportional to the energy that is dissipated in each cycle [42, 43]. Figures 6 and 7 show the frequency dependence of dielectric constant and dielectric, loss respectively, at selected temperatures for chitosan-$LiCF_3SO_3$, chitosan-$NaCF_3SO_3$, and chitosan-$AgCF_3SO_3$ membranes. At low frequency, due to the long period and thus showing reversal of the electrical field, the mobile ions tend to accumulate at the electrode/solid electrolyte interface. This gives a high value of dielectric constant (ε') and dielectric loss (ε''). On the other hand, at high frequencies, periodic reversal of the electric field occurs so fast that there is no excess ion diffusion in the direction of the field. Polarization due to charge accumulation decreases, leading to the observed decrease in dielectric constant and dielectric loss [44].

It is obvious (Figures 6 and 7) that dielectric constant and dielectric loss increase at high temperatures due to the higher charge carrier density. As temperature increases, the degree of salt dissociation and redissociation of ion aggregates increases [40], as a result of the decrease in bond energies with temperature [45]. Consequently the numbers of free ions or charge carrier density increase. Ramya et al. [46] reported that the increase in the dielectric constant represents a fractional increase in charges within the polymer electrolyte. The dependence of charge carrier concentration n upon the dissociation energy U and dielectric constant ε can be explained through the relation, $n = n_o \exp(-U/\varepsilon kT)$, where k is the Boltzmann constant and T is the absolute temperature. Thus, the higher value in dielectric constant and dielectric loss at high temperatures indicates an increase in carrier concentration, that is, an increase in conductivity.

The observed power law dispersion in ε'' spectra (Figure 6) and the absence of relaxation peaks indicate the dc contribution. This indicates that ionic and polymer segmental motions are strongly coupled. It can be noticed that the chitosan: $AgCF_3SO_3$ membrane exhibits higher dielectric constant and dielectric loss compared to chitosan: $LiCF_3SO_3$ and chitosan: $NaCF_3SO_3$ membranes. This is due to the fact that amorphous regions make the major contribution to both dielectric constant (ε') and dielectric loss (ε'') [47]. Thus, the high amorphous and high ionic transport indicate that chitosan: $AgCF_3SO_3$ membrane is a good candidate as a solid polymer electrolyte membrane for facilitated olefin carrier transport membranes as the other polymers such as poly(ethylene phthalate) (PEP), poly(ethylene oxide) (PEO), poly(2-ethyl-2-oxazoline) (POZ), or poly(vinyl pyrrolidone) (PVP) [48].

4. Conclusion

The influence of cation size on the chitosan structure has been investigated by X-ray diffraction. It was found that the intensity of the crystalline peak of pure chitosan decreased with increasing cation size. This is due to the stability of complexes formed between Lewis acids and bases. It was found that chitosan-$AgCF_3SO_3$ membrane exhibits high amorphous nature and the XRD results confirm that the effect of cation size on the crystalline nature of chitosan membrane has the following order: $LiCF_3SO_3$ < $NaCF_3SO_3$ < $AgCF_3SO_3$. The small radius of the Z''-Z' curve for chitosan-$AgCF_3SO_3$ compared to the other two solid electrolytes can be attributed to high conductivity (ionic transport). The appearance of a peak at 412 nm in the UV-vis spectra confirms the formation of silver metal nanoparticles in chitosan-$AgCF_3SO_3$ system. The high value of dielectric constant and dielectric loss of chitosan-$AgCF_3SO_3$ is attributed to the dominance of amorphous nature of the sample. The increase of dielectric constant and dielectric loss with temperature for chitosan-salt systems indicates the increase of charge carrier concentration. The absence of peak in dielectric loss (ε'') spectra can be attributed to dc contribution and a well-coupling between polymer segmental and ionic motions.

Conflict of Interests

Shujahadeen B. Aziz and Zul Hazrin Z. Abidin confirm that there is no known conflict of interests associated with this paper and there has been no significant financial support for this work that could have influenced its outcome.

Acknowledgments

The authors gratefully acknowledge the grant from University of Malaya (Grant no. PS214/2009A) for this research project. Shujahadeen Bakr Aziz wishes to thank the Ministry of Higher Education and Scientific Research-Kurdistan Regional Government for the scholarship awarded and Ahmed Esmael Nanakaly for financial support.

References

[1] G. Rajasudha, L. M. Jayan, D. Durga Lakshmi et al., "Polyindole-CuO composite polymer electrolyte containing $LiClO_4$ for lithium ion polymer batteries," *Polymer Bulletin*, vol. 68, no. 1, pp. 181–196, 2012.

[2] A. M. Stephan, "Review on gel polymer electrolytes for lithium batteries," *European Polymer Journal*, vol. 42, no. 1, pp. 21–42, 2006.

[3] S. Zhou and S. Fang, "High ionic conductivity of all-solid polymer electrolytes based on polyorganophosphazenes," *European Polymer Journal*, vol. 43, no. 8, pp. 3695–3700, 2007.

[4] A. Bhide and K. Hariharan, "Ionic transport studies on $(PEO)_6$:$NaPO_3$ polymer electrolyte plasticized with PEG400," *European Polymer Journal*, vol. 43, no. 10, pp. 4253–4270, 2007.

[5] W. Li, M. Yuan, and M. Yang, "Dual-phase polymer electrolyte with enhanced phase compatibility based on Poly(MMA-g-PVC)/PMMA," *European Polymer Journal*, vol. 42, no. 6, pp. 1396–1402, 2006.

[6] H. Mitsuda, T. Uno, M. Kubo, and T. Itoh, "Solid polymer electrolytes based on poly(1,3-diacetyl-4-imidazolin-2-one)," *Polymer Bulletin*, vol. 57, no. 3, pp. 313–319, 2006.

[7] P.-L. Kuo, W.-J. Liang, and T.-Y. Chen, "Solid polymer electrolytes V: microstructure and ionic conductivity of epoxide-crosslinked polyether networks doped with $LiClO_4$," *Polymer*, vol. 44, no. 10, pp. 2957–2964, 2003.

[8] C. Tan, W. He, H. Meng, and X. Huang, "A novel titration method based on fiber-optic refractive index sensing for the determination of deacetylation degree of chitosans," *Polymer Bulletin*, vol. 69, pp. 189–197, 2012.

[9] P. Agrawal, G. J. Strijkers, and K. Nicolay, "Chitosan-based systems for molecular imaging," *Advanced Drug Delivery Reviews*, vol. 62, no. 1, pp. 42–58, 2010.

[10] P. Bai, F. Cao, X. Lan, F. Zhao, Y. Ma, and C. Zhao, "Chitosan gel beads immobilized Cu (II) for selective adsorption of amino acids," *Journal of Biochemical and Biophysical Methods*, vol. 70, no. 6, pp. 903–908, 2008.

[11] G. Lu, L. Kong, B. Sheng, G. Wang, Y. Gong, and X. Zhang, "Degradation of covalently cross-linked carboxymethyl chitosan and its potential application for peripheral nerve regeneration," *European Polymer Journal*, vol. 43, no. 9, pp. 3807–3818, 2007.

[12] S. L. Agrawal, M. Singh, M. Tripathi, M. M. Dwivedi, and K. Pandey, "Dielectric relaxation studies on [PEO-SiO_2]:NH_4SCN nanocomposite polymer electrolyte films," *Journal of Materials Science*, vol. 44, no. 22, pp. 6060–6068, 2009.

[13] S. B. Aziz and Z. H. Z. Abidin, "Electrical conduction mechanism in solid polymer electrolytes: new concepts to arrhenius equation," *Journal of Soft Matter*, vol. 2013, Article ID 323868, 8 pages, 2013.

[14] F. Yuan, Z. Peng, and J.-M. Liu, "Dielectric behaviors of relaxor ferroelectric $Pb(Mg_{1/2}Nb_{1/2})O_3$–35% $PbTiO_3$: temperature and frequency dependences," *Materials Science and Engineering B*, vol. 117, no. 3, pp. 265–270, 2005.

[15] S. B. Aziz, "Li^+ ion conduction mechanism in poly (ε-caprolactone)-based polymer electrolyte," *Iranian Polymer Journal*, vol. 22, pp. 877–883, 2013.

[16] S. B. Aziz, Z. H. Z. Abidin, and A. K. Arof, "Effect of silver nanoparticles on the DC conductivity in chitosansilver triflate polymer electrolyte," *Physica B*, vol. 405, no. 21, pp. 4429–4433, 2010.

[17] J. Malathi, M. Kumaravadivel, G. M. Brahmanandhan, M. Hema, R. Baskaran, and S. Selvasekarapandian, "Structural, thermal and electrical properties of PVA-$LiCF_3SO_3$ polymer electrolyte," *Journal of Non-Crystalline Solids*, vol. 356, pp. 2277–2281, 2010.

[18] K. C. Khulbe, T. Matsuura, G. Lamarche, and A.-M. Lamarche, "X-ray diffraction analysis of dense PPO membranes," *Journal of Membrane Science*, vol. 170, no. 1, pp. 81–89, 2000.

[19] R. P. Suvarna, K. R. Rao, and K. Subbarangaiah, "A simple technique for a.c. conductivity measurements," *Bulletin of Materials Science*, vol. 25, no. 7, pp. 647–651, 2002.

[20] A. S. A. Khiar, R. Puteh, and A. K. Arof, "Conductivity studies of a chitosan-based polymer electrolyte," *Physica B*, vol. 373, no. 1, pp. 23–27, 2006.

[21] K. P. Padmasree and D. K. Kanchan, "Modulus studies of CdI_2-Ag_2O-V_2O_5-B_2O_3 system," *Materials Science and Engineering B*, vol. 122, no. 1, pp. 24–28, 2005.

[22] S. Rajendran, R. S. Babu, and P. Sivakumar, "Investigations on PVC/PAN composite polymer electrolytes," *Journal of Membrane Science*, vol. 315, no. 1-2, pp. 67–73, 2008.

[23] F. Göktepe, S. Ü. Çelik, and A. Bozkurt, "Preparation and the proton conductivity of chitosan/poly(vinyl phosphonic acid) complex polymer electrolytes," *Journal of Non-Crystalline Solids*, vol. 354, no. 30, pp. 3637–3642, 2008.

[24] Y. Wan, K. A. M. Creber, B. Peppley, and V. Tam Bui, "Chitosan-based solid electrolyte composite membranes—I. Preparation and characterization," *Journal of Membrane Science*, vol. 280, no. 1-2, pp. 666–674, 2006.

[25] B. Smitha, S. Sridhar, and A. A. Khan, "Chitosan-sodium alginate polyion complexes as fuel cell membranes," *European Polymer Journal*, vol. 41, no. 8, pp. 1859–1866, 2005.

[26] S. A. Hashmi and S. Chandra, "Experimental investigations on a sodium-ion-conducting polymer electrolyte based on poly(ethylene oxide) complexed with NaPF6," *Materials Science and Engineering B*, vol. 34, no. 1, pp. 18–26, 1995.

[27] R. A. Sanders, A. G. Snow, R. Frech, and D. T. Glatzhofer, "A spectroscopic and conductivity comparison study of linear poly(N-methylethylenimine) with lithium triflate and sodium triflate," *Electrochimica Acta*, vol. 48, no. 14–16, pp. 2247–2253, 2003.

[28] M. Hema, S. Selvasekarapandian, D. Arunkumar, A. Sakunthala, and H. Nithya, "FTIR, XRD and ac impedance spectroscopic study on PVA based polymer electrolyte doped with NH_4X(X = Cl, Br, I)," *Journal of Non-Crystalline Solids*, vol. 355, no. 2, pp. 84–90, 2009.

[29] P. B. Bhargav, V. M. Mohan, A. K. Sharma, and V. V. R. N. Rao, "Investigations on electrical properties of (PVA:NaF) polymer electrolytes for electrochemical cell applications," *Current Applied Physics*, vol. 9, no. 1, pp. 165–171, 2009.

[30] S. Sunderrajan, B. D. Freeman, C. K. Hall, and I. Pinnau, "Propane and propylene sorption in solid polymer electrolytes based on poly(ethylene oxide) and silver salts," *Journal of Membrane Science*, vol. 182, no. 1-2, pp. 1–12, 2001.

[31] I. Pinnau and L. G. Toy, "Solid polymer electrolyte composite membranes for olefin/paraffin separation," *Journal of Membrane Science*, vol. 184, no. 1, pp. 39–48, 2001.

[32] R. J. Sengwa and S. Sankhla, "Characterization of ionic conduction and electrode polarization relaxation processes in ethylene glycol oligomers," *Polymer Bulletin*, vol. 60, no. 5, pp. 689–700, 2008.

[33] D. K. Pradhan, R. N. P. Choudhary, and B. K. Samantaray, "Studies of structural, thermal and electrical behavior of polymer nanocomposite electrolytes," *Express Polymer Letters*, vol. 2, no. 9, pp. 630–638, 2008.

[34] A. Bakker, S. Gejji, J. Lindgren, K. Hermansson, and M. M. Probst, "Contact ion pair formation and ether oxygen coordination in the polymer electrolytes $M[N(CF_3SO_2)_2]_2PEOn$ for M = Mg, Ca, Sr and Ba," *Polymer*, vol. 36, no. 23, pp. 4371–4378, 1995.

[35] S. W. Kang, J. H. Kim, K. S. Oh et al., "Highly stabilized silver polymer electrolytes and their application to facilitated olefin transport membranes," *Journal of Membrane Science*, vol. 236, no. 1-2, pp. 163–169, 2004.

[36] P. Y. Lim, R. S. Liu, P. L. She, C. F. Hung, and H. C. Shih, "Synthesis of Ag nanospheres particles in ethylene glycol by electrochemical-assisted polyol process," *Chemical Physics Letters*, vol. 420, no. 4-6, pp. 304–308, 2006.

[37] J. H. Kim, B. R. Min, J. Won, and Y. S. Kang, "Anomalous temperature dependence of facilitated propylene transport in silver polymer electrolyte membranes," *Journal of Membrane Science*, vol. 227, no. 1-2, pp. 197–206, 2003.

[38] J. H. Kim, C. K. Kim, J. Won, and Y. S. Kang, "Role of anions for the reduction behavior of silver ions in polymer/silver salt complex membranes," *Journal of Membrane Science*, vol. 250, no. 1-2, pp. 207–214, 2005.

[39] S. H. Mun, S. W. Kang, J.-S. Cho, S.-K. Koh, and Y. S. Kang, "Enhanced olefin carrier activity of clean surface silver nanoparticles for facilitated transport membranes," *Journal of Membrane Science*, vol. 332, no. 1-2, pp. 1–5, 2009.

[40] M. Selva Kumar and D. K. Bhat, "Polyvinyl alcohol-polystyrene sulphonic acid blend electrolyte for supercapacitor application," *Physica B*, vol. 404, no. 8–11, pp. 1143–1147, 2009.

[41] D. K. Pradhan, R. N. P. Choudhary, and B. K. Samantaray, "Studies of dielectric relaxation and AC conductivity behavior of plasticized polymer nanocomposite electrolytes," *International Journal of Electrochemical Science*, vol. 3, pp. 597–608, 2008.

[42] M. Okutan and E. Şentürk, "β Dielectric relaxation mode in side-chain liquid crystalline polymer film," *Journal of Non-Crystalline Solids*, vol. 357, pp. 1526–1530, 2008.

[43] K. M. Batoo, S. Kumar, C. G. Lee, and A. Alimuddin, "Study of dielectric and ac impedance properties of Ti doped Mn ferrites," *Current Applied Physics*, vol. 9, no. 6, pp. 1397–1406, 2009.

[44] C. V. Subba Reddy, X. Han, Q.-Y. Zhu, L.-Q. Mai, and W. Chen, "Dielectric spectroscopy studies on (PVP + PVA) polyblend film," *Microelectronic Engineering*, vol. 83, no. 2, pp. 281–285, 2006.

[45] M. S. Salem, *Journal of Material Science*, vol. 44, p. 5660, 2009.

[46] C. S. Ramya, S. Selvasekarapandian, G. Hirankumar, T. Savitha, and P. C. Angelo, "Investigation on dielectric relaxations of PVP-NH_4SCN polymer electrolyte," *Journal of Non-Crystalline Solids*, vol. 354, no. 14, pp. 1494–1502, 2008.

[47] K. C. Kwan, *Dielectric Phenomena in Solids*, Elsevier Academic Press, 2004.

[48] S. B. Aziz, Z. H. Z. Abidin, and A. K. Arof, "Influence of silver ion reduction on electrical modulus parameters of solid polymer electrolyte based on chitosan-silver triflate electrolyte membrane," *eXPRESS Polymer Letters*, vol. 4, no. 5, pp. 300–310, 2010.